


**Please cite the Published Version**

Jesson, Michael, Sterling, Mark  and Bridgeman, John (2013) Despiking velocity time-series-Optimisation through the combination of spike detection and replacement methods. Flow Measurement and Instrumentation, 30. pp. 45-51. ISSN 0955-5986

**DOI:** <https://doi.org/10.1016/j.flowmeasinst.2013.01.007>

**Publisher:** Elsevier BV

**Version:** Accepted Version

**Downloaded from:** <https://e-space.mmu.ac.uk/634431/>

**Usage rights:**  [Creative Commons: Attribution-Noncommercial-No Derivative Works 4.0](https://creativecommons.org/licenses/by-nc-nd/4.0/)

**Additional Information:** © 2013. This manuscript version is made available under the CC-BY-NC-ND 4.0 license <https://creativecommons.org/licenses/by-nc-nd/4.0/>

**Enquiries:**

If you have questions about this document, contact [openresearch@mmu.ac.uk](mailto:openresearch@mmu.ac.uk). Please include the URL of the record in e-space. If you believe that your, or a third party's rights have been compromised through this document please see our Take Down policy (available from <https://www.mmu.ac.uk/library/using-the-library/policies-and-guidelines>)

This post-print version is released under a Creative Commons Attribution Non-Commercial No  
Derivatives License (see <http://creativecommons.org/licenses/by-nc-nd/4.0/>).

The published version may be accessed from:

[Jesson, M., Sterling, M., Bridgeman, J., 2013. Despiking Velocity Time-Series – Optimisation Through the Combination of Spike Detection and Replacement Methods. \*Flow Measurement and Instrumentation\* 30, 45–51. doi:10.1016/j.flowmeasinst.2013.01.007](#)

# **Despiking Velocity Time-Series – Optimisation Through the Combination of Spike Detection and Replacement Methods**

Michael Jesson \*

Mark Sterling

John Bridgeman

School of Civil Engineering, The University of Birmingham, Edgbaston, Birmingham, B15 2TT, United Kingdom +44 (0) 121 414 5145, Fax: +44 (0) 121 414 3675

\* Corresponding author: m.a.jesson@bham.ac.uk

## **Abstract**

The experimental investigation of turbulence has been greatly aided by the development of instruments capable of measuring and recording instantaneous velocity measurements at high frequencies, such as Laser Doppler and Acoustic Doppler Velocimeters. As a consequence of the techniques and algorithms used by some of these instruments, the introduction of 'spikes' of invalid data into the recorded velocity time-series is inevitable, with resulting errors in the calculated turbulence characteristics. These spikes should, therefore, be removed and replaced with statistically valid values if power spectra and parameters such as turbulence intensity are to be examined. A number of existing spike detection and replacement methods are discussed and combinations of these have been applied to data from a variety of sources - artificially corrupted test data, data from laboratory experiments in a flume and data from field experiments in a natural river. Earlier recommendations, based on studies using a smaller number of despiking methods and data sources, are improved; contrary to previous findings, Phase-Space Thresholding is shown to accurately reconstruct the power spectrum when used with the appropriate replacement method.

# 1 Introduction

Instruments capable of recording high frequency velocity time-series have revolutionised the study of turbulence, allowing direct calculation of parameters such as Reynolds stress and power spectra. It is clear, however, that such calculations are only valid if the time-series are an accurate record of the instantaneous velocities. Further, certain instruments (such as Laser Doppler Velocimeters (LDVs) and Acoustic Doppler Velocimeters (ADV)) have been shown to introduce 'spikes' of invalid data into the time-series under certain conditions (see, for example, [1], [2]). The identification and removal of such spikes thus becomes an important part of the post-processing of such data, prior to its use in turbulence studies.

The algorithms discussed in this paper are based purely on the statistical properties of the time-series and are in no way dependent on the instrument which recorded them. As such they may be applied to any velocity time-series, but are discussed here in reference to ADV data for two reasons: firstly, the algorithms were developed to process ADV data, and secondly the majority of the authors' experience in this area is in the deployment of ADVs. Readers with a particular interest in LDV applications are directed to the excellent overview papers of Tropea [1] and Benedict et al. [3]. The Acoustic Doppler Velocimeter (ADV) was developed by the US Army Engineer Waterways Experiment Station to provide an instrument capable of giving instantaneous velocity measurements in three dimensions [4]. Modern ADVs are capable of sampling at a rate of 200Hz [5], allowing the capture of turbulent velocity fluctuations in addition to mean velocities, while their small size and portability make them a useful tool for both laboratory and field experimental work (see, for example, [6-8]).

The measurements obtained from an ADV can be compromised by a number of issues which affect their accuracy. The salinity and temperature of the water affect the speed of sound, leading to errors of over 3% for an uncalibrated probe [4]. Doppler noise, an approximately Gaussian white-noise [9], is inherent in any device which uses Doppler backscattering to calculate velocities [4]. The cause of

this noise is not fully understood, but it is thought that there are three main causes: particles entering and leaving the sampling volume during the interval between pulses, turbulence at scales smaller than the measuring volume, and beam divergence [9]. Similar causes of spikes have been identified for LDVs [1].

The ADV measures velocities using the principal of Doppler shift, where sound waves bounced off a moving object (in this case a particle carried in the water) undergo a phase shift which is proportional to the velocity of the object. This phase shift can only be measured within the range -180° to +180°, with any shift outside of this range leading to a spike in the velocity time-series in a phenomenon known as aliasing [2, 10]. The authors have also found that, in a laboratory environment where the lack of impurities in the water necessitates the use of a bubble generator to create bubbles to reflect the ADV sound waves (see [11] for details), instants of low bubble density may also cause spikes.

It is the detection, removal and replacement of such spikes which is the subject of this paper; example velocity time-series (both pre- and post-filtering) spikes are shown in Figure 1. A number of detection methods have been developed by other researchers, such as the Phase-Space Thresholding method (PST) of Goring and Nikora [2] and its variant, the modified PST (mPST) of Parsheh et al. [12]. Both teams recommend schemes for estimating a value with which to replace the spike and maintain the length of the time-series, but the choice is somewhat arbitrary. To the authors' knowledge the effect of different combinations of detection and replacement method have not been examined in detail under application to both artificially contaminated test data and real experimental data. In light of the work of Parsheh et al. [12], who found issue with the reconstruction of power spectra when using PST with their chosen replacement method, this is seen as an important area of investigation, particularly with respect to existing data sets which may have been processed using PST.

Relevant detection and replacement schemes are described in the following sections, after which the result of their application to a number of data sets is presented. Finally, conclusions which may be drawn from this work are identified.

## 2 Methods and Test Data

### 2.1 Filtering Methods and Replacement Methods

The problem of spike removal lies in determining which of the data points are, in fact, spikes and the best method of replacing spikes with estimated values. This is non-trivial, and a number of different filtering methods and different replacement methods have been suggested. Any filtering method may be used in conjunction with any replacement method - herein, any such combination of a filtering method and a replacement method is termed a despiking method. The Phase-Space Threshold (PST) filtering method of Goring and Nikora [2] has become a *de facto* standard for the filtering of ADV data, and has been modified in an attempt to further improve the method (for example, [13] and [12]) and been an inspiration for other methods such as the Velocity Correlation method [14]. PST and other pertinent filtering methods are described below. Instantaneous velocity components in the  $x$ ,  $y$  and  $z$  directions are referred to as  $u$ ,  $v$  and  $w$  respectively, with primes (e.g.  $u'$ ) representing turbulent fluctuations.

#### 2.1.1 Phase-Space Threshold (PST)

Goring and Nikora [2] developed a method based on phase-space plots of the turbulent velocity fluctuations,  $u'$ , and their first and second derivatives,  $\Delta u'$  and  $\Delta^2 u'$  respectively.  $\Delta u'$  and  $\Delta^2 u'$  are approximated from the discrete time-series of  $u'$  using the central difference method:

$$\Delta u'_i \cong u'_{i+1} - u'_{i-1} \quad (1)$$

$$\Delta^2 u'_i \cong \Delta u'_{i+1} - \Delta u'_{i-1} \equiv u'_{i+2} - u'_{i-2} \quad (2)$$

where  $i$  indexes the time-series (note that the factor  $1/\Delta t$ , where  $\Delta t$  is the time-step between measurements, is intentionally omitted without affecting the filtering [2]). Three plots are obtained,

$u'-\Delta u'$ ,  $u'-\Delta^2 u'$  and  $\Delta u'-\Delta^2 u'$ , in each of which those points which lie outside of a prescribed ellipse are deemed invalid. Taking the  $u'-\Delta u'$  plot as an example, the co-ordinates of the centre of the ellipse are the means of  $u'$  and  $\Delta u'$ , while the length of the ellipse axes:

$$l_u = \lambda \sigma_u \quad l_{\Delta u} = \lambda \sigma_{\Delta u} \quad (3)$$

are the product of the universal threshold:

$$\lambda = \sqrt{2 \ln(N)} \quad (4)$$

(where  $N$  is the number of measurements in the sample) and the respective standard deviation,  $\sigma_u$  or  $\sigma_{\Delta u}$ . The axes length therefore represent the expected absolute maxima of  $u'$  and  $\Delta u'$  [2]. The median absolute deviation,  $\vartheta$ , has been identified as a more accurate measure of true variation in a time-series corrupted by large magnitude spikes and may be used as an alternative to  $\sigma$  in (3) [13]. In the context of (3),  $\sigma$  or  $\vartheta$  is herein referred to as the characteristic scalar (CS).

### 2.1.2 Modified Phase-Space Threshold (mPST)

As spikes are frequently of a much greater magnitude than the valid data there is a tendency for the original PST method to incorrectly identify valid measurements adjacent to spikes as invalid due to the high value of  $\Delta u'_i$  arising from (1), which includes the spike value. In order to overcome this, Parsheh et al. [12] suggest a modified version in which user-specified constants,  $C_1$  and  $C_2$  are used to flag measurements as valid (and therefore never to be identified as spikes) if  $-C_1 \vartheta_u \leq u' \leq C_1 \vartheta_u$  and to be excluded if  $|u'| > C_2 \vartheta_u \lambda$ . The latter,  $C_2$ , condition is used to pre-filter the data before the standard PST method is applied, while the former,  $C_1$ , condition is used for each measurement on each iteration of the algorithm.

### 2.1.3 Velocity Correlation (VC)

An alternative filtering method, the Velocity Correlation Filter, was suggested and compared to the PST by Cea et al. [14]. This uses the filtering ellipse as for PST, but differs by plotting the three velocity components against each other (in the  $u'-v'$ ,  $u'-w'$  and  $v'-w'$  planes) rather than filtering

each velocity component separately against its own derivatives. No data is replaced during the filtering, and mean flow statistics are calculated before any replacement is done – unlike most of the other methods, it is not iterative. Cea et al. considered this non-iterative approach to be likely to give better results with highly turbulent flows (in particular, they were investigating the flow in fishway), but noted that this method loses the benefits of differentiation of the velocity signal which enhances high-frequency components and thus aids spike identification.

## **2.2 Replacement Methods**

Once a spike has been detected it may (when a complete time-series is required) be replaced by an approximated value, and a number of methods for calculating the replacement value have been suggested (see [2], for example), with relevant methods discussed below. It should be noted that these methods are not intended to estimate the particular value which was obliterated by the spike; rather they aim to replace the spike with a value which is statistically valid within the time-series as a whole. While no single method may be considered more accurate than another in terms of calculating replacement values from valid values (though, as Goring and Nikora [2] note, some are more “*aesthetically pleasing*” than others), spikes which have not yet been removed may affect these replacement methods – this is discussed further as each method is described.

### **2.2.1 Last Good Value (LGV)**

Any spike is simple replaced with the last good (valid) value. This method has the advantage of being independent of the values surrounding the spike (which may themselves be spikes). However, bearing in mind that the filtering methods are iterative processes, this is also a disadvantage as the last “good” value may itself be a spike which would be removed on subsequent iterations. If this occurs for a relatively large number of spikes then the effect on the mean and standard deviations may be non-negligible, though this could possibly be mitigated by, for the second and subsequent iterations, ignoring the replaced values when calculating these parameters (the effects of such a change to the filtering method are not considered in this paper).



### **2.2.2 Linear Interpolation (LI)**

The replacement value is calculated by simple linear interpolation between the valid values surrounding the spike. If one of the surrounding values is a yet-to-be-removed spike the replacement value may constitute a spike. Potentially, if the first derivative would have identified the true spike, the replacement value may reduce  $\Delta u'$  to within valid values, hiding the true spike for subsequent iterations.

### **2.2.3 12-Point Polynomial (12PP)**

The favoured method of Goring and Nikora [2], the best-fit cubic polynomial for the 12 valid points either side of the spike (i.e. 24 points in total) is calculated and its value at the spike used as the replacement value. Although spikes may span a number of consecutive measurements, the spike duration is generally small (in artificially corrupting the data discussed in Section 2.3, for example, Parsheh et al. [12] limit their spike duration to a maximum of 4 measurements) and so yet-to-be-removed spikes would be expected to have little effect on the 12PP replacement method. While the work of Parsheh et al. has resulted in the development of an effective, computationally efficient despiking method, they have neglected the 12PP replacement method in their analysis, an issue which this paper addresses.

## **2.3 Test Data and its Despiking**

The data examined for this study came from three sources. In the development of the mPST, Parsheh et al. [12] made use of a “clean” set of 1.2 million instantaneous  $u$  velocities (hot-wire anemometer (HWA) measurements made in the turbulent boundary layer over a rough surface in a wind tunnel, at a rate of 20kHz) which was artificially contaminated with spikes (replacing 5% of the valid values), providing an easily verifiable test case. A copy of this data, which is described more fully by Parsheh et al. [12], was kindly supplied to the authors. This data has been used both in its entirety and also to provide a smaller (100,000 velocities) data set which proved more practical when performing computationally intensive calculations on the PC used for the data processing. The

second data source was the experimental data gathered by the authors in their investigation of open-channel flow in a heterogeneous channel, fully described in [15]. Briefly, uniform, sub-critical, flow conditions were set in a 22m long, 0.61m wide, inclined experimental flume. The bed roughness was laterally heterogeneous, with sections of smooth PVC sheeting and of gravel. The data consist of instantaneous, 3-D, velocity measurements made at a rate of 200Hz using a Nortek ADV, with the nominal velocity range set to  $\pm 0.3\text{ms}^{-1}$  (this gives a horizontal range of  $0.94\text{ms}^{-1}$ ; see [16] for details), and a sampling volume of 7mm. Measurements were made at over 500 data points spanning a cross-section of the channel, with the velocity at each data point sampled for a duration of 60s (i.e. 12,000 velocity measurements per data point). The third source was Gunawan et al. [17], who provided seven sets of 25Hz Nortek ADV data gathered in field experiments in the River Blackwater in the South of England - again, the sharing of this data is much appreciated. Using these three sources enables the despiking methods to be evaluated against data gathered in different scenarios – idealised corruption for test, laboratory flume experiments with clean, treated water, and field experiments with dirty, untreated river water.

The despiking was performed using a Java application developed by the authors for the batch analysis of their large quantities (5000+ time-series, each of 60s length) of experimental data described in [15] and [8]. This software will read multiple data files, each containing the measurements for a single data point, and plot the data over a channel cross-section, and is freely downloadable from [www.mikejesson.com](http://www.mikejesson.com). Among other functionality, the application can be configured to despike the data with the filtering and replacement methods selectable from a number of options, including those described above.

### **3 Results and Discussion**

#### **3.1 The Full Data Set of Parsheh et al.**

The accuracy of the despiking methods is evaluated by counting the number of spikes correctly identified, the number of spikes missed and the number of valid data points incorrectly identified as

spikes (Table 1). The standard deviation of the despiked series is also included in this table, and clearly should approximate the standard deviation of the uncontaminated data. However, as a simple example, consider the series 4.4, 4.6, 4.7, 4.5. If 4.7 is taken to be a spike then LGV replacement gives  $\sigma = 0.096$  for the despiked series, whereas LI replacement gives  $\sigma = 0.086$ . If the real value were 4.6 then LGV would more accurately reconstruct the standard deviation; if the real value were 4.5 then LI would give a more accurate reconstruction – either value is statistically equally likely and so, certainly from a single data set, the precise value of the standard deviation is not a suitable parameter for comparison of despiking methods.

Of the filtering methods described above only mPST has been applied successfully to the full data set using  $\sigma$  as the CS in (3). When  $\sigma$  was used with PST (as in the original algorithm of Goring and Nikora [2]), the algorithm continued to identify spikes after a large number of iterations. Inspection of the data during the processing showed that far more spikes had been identified than the number of true spikes. Using  $\vartheta$  as the CS allowed PST-12PP to be applied to the full data set, termed PST- $\vartheta$ -12PP, but PST- $\vartheta$ -LGV failed. For mPST, the values  $C_1 = 1.8$  and  $C_2 = 1.35$  were used, as recommended by Parsheh et al. [12], with each of the replacement methods described above. As may be seen from Table 1, in terms of correctly identifying real spikes there is negligible difference between the three mPST despiking methods (mPST-12PP, mPST-LGV and mPST-LI), with 99.8% of the spikes identified. Surprisingly, mPST-LI performs significantly better in terms of the number of measurements incorrectly identified as spikes, though even in the worst case (mPST-LGV) the number of incorrectly identified spikes is only 1% of the number of correctly identified spikes, and 0.05% of the total number of measurements. PST- $\vartheta$ -12PP detects all spikes, but this must be partly ascribed to the removal of four times as many “spikes” as are actually in the contaminated data set. The velocity correlation filter fails to identify approximately 4000 spikes, though it should be noted that this data set is single component and so the VC method reduces to being an upper limit on the  $u$  fluctuations.

As is shown in Section 3.2, the application of PST to the partial (100,000 data point) data set was more successful. The failure of PST therefore appears to be related to the length of the time-series and, therefore, the universal threshold defined in (4). The partial data set and full data set are statistically equivalent (the mean value differs by <2% while the standard deviations are negligibly different), and so, for the first iteration, the axes lengths will differ by the ratio  $(\ln(N_{full})/\ln(N_{partial}))^{1/2}$ . Hence proportionally more spikes will be removed per iteration for smaller  $N$ , reducing the number of iterations required to remove all spikes. This reduction in iterations will be increased since, for subsequent iterations, the CS will be of lesser magnitude for smaller  $N$  due to the removal of a greater percentage of the spikes, further reducing the axes lengths. From this analysis it is predicted that, given sufficient time/processing power the other PST despiking methods would also succeed. This is supported by the comparison of the PST- $\vartheta$ -12PP results from the full and partial (see Table 2) data sets, which show that for  $N_{partial} = N_{full}/12$  the removal counts are approximately 1/12 of those seen for the full data set.

### 3.2 The Partial Data Set of Parsheh et al.

A 100,000 measurement sub-set of the data of Parsheh et al. was filtered using mPST and PST in combination with the three replacement methods and the two CS options (Table 2). Although use of  $\vartheta$  as the CS is more robust, the results indicate that its use increases the number of valid measurements identified as spikes.  $\sigma$  would therefore be the recommended default CS, with  $\vartheta$  used if necessary to aid the iterative process.

When using PST, the number of valid values identified as spikes is (at least) approximately equal to the number of correctly replaced spikes, whereas with mPST it is negligible. However, further investigation suggests that the properties of the data set are somewhat skewing this analysis.  $\sigma$  and  $\vartheta$  were calculated before and after the initial mPST automatic exclusion step (i.e. application of the  $C_2$  condition), and the number of removed values noted (Table 3). For the data of Parsheh et al., approximately 3% of the values are removed at this stage, with  $\sigma$  falling by approximately 60% as a

result. Further, this new value of  $\sigma$  (which, under the standard algorithm, is now the CS) is approximately equal to the value of  $\vartheta$  before the exclusion. With the experimental data of Jesson et al. this automatic exclusion step has a much smaller effect, with only 0.4% of the values removed and  $\sigma$  reducing by only 12% (note that the figures given for Jesson et al. in Table 3 are the mean values over all data points in their data set). The values of  $\vartheta$  and  $\sigma$  at the start of the process are also much closer (approximately 16% difference) than those for Parsheh et al., and so the choice of CS would be expected to have a much lesser effect in this case. Thus, while the data of Parsheh et al. provides a useful, clean data set for validation of mPST and comparison of the replacement methods and choice of CS, the authors feel that analysis based on this data set may exaggerate the limitations of PST (this is not intended as a criticism of mPST, which is the authors' preferred filtering method due to its efficiency, but rather a defence of PST). It should be emphasised that this difference is due to the method of corrupting the data of Parsheh et al., rather than a feature of HWA measurements when compared to ADV measurements.

Parsheh et al. [12] focussed on the despiking of ADV data for the purpose of estimating power spectra, and showed that mPST-LGV (mPST-SH in their notation) vastly improved the estimation in comparison to PST-LI. This was demonstrated for both the data set described here and a second set of intentionally contaminated ADV data. A similar analysis has been performed using the Fourier transform into the frequency domain,  $F(f)$ , (where  $f$  is the frequency), of the time-series to give an approximation to the spectral energy function,  $S(k)$ , where  $k = 2\pi f/U$  is the wavenumber and:

$$S(k) \cong \frac{U}{2\pi} F(f) \quad (5)$$

as described by Nezu and Nakagawa [18]. It should be noted that (5) is only applicable when Taylor's frozen turbulence hypothesis holds, an assumption which the authors feel is reasonable for the steady-state conditions under which the data were gathered. It may be seen (Figure 2) that both PST-12PP and mPST-LGV accurately reconstruct the power spectrum except at high frequencies, while mPST-12PP diverges from the uncontaminated power spectrum at a much lower frequency. It

is interesting to note that the (unshown) power spectrum for PST-LGV follows the mPST-12PP spectrum, i.e. the each of the two replacement methods appears to be compatible with a different filtering method. Further, if  $C_1$  is set to 0 (i.e. there are no points marked as valid) the mPST-12PP spectrum falls on the PST-12PP spectrum, while if  $C_2$  is set to 0 (causing the software to not automatically exclude any points before starting the PST iterations) the mPST-12PP spectrum is unchanged (not shown) – it would appear that the  $C_1$  condition is more influential change to the standard PST algorithm.

### 3.3 The Data of Jesson et al.

As shown earlier, the data set of Parsheh et al. is statistically very different to the experimental data gathered by Jesson et al.. Further, the sets of experimental data examined by Parsheh et al. (ADV measurements deliberately corrupted via non-optimal configuration of the ADV [12]) are highly corrupted (10%-25% spikes). Applying the various despiking methods to the data of Jesson et al. shows that PST identifies approximately twice as many values as being spikes than mPST or VC (Table 4). In this table, the mPST-LGV value of the turbulence intensity (TI) components is taken as the baseline and values are mean values over all of the data points forming the data set. The variation in TI is seen to be small, though PST-LGV increases the z-component of TI,  $TI_z$ , by 4% relative to mPST-LGV. The PST-LGV  $TI_z$  is therefore greater than that for the unfiltered data. This may appear erroneous but it should be noted that if a  $u$  measurement is identified as a spike then the corresponding  $v$  and  $w$  measurements are also replaced, potentially by a value with a larger fluctuation from the mean than the original if LGV is used.

In order to examine the despiking method output for individual data points,  $TI_x$  was calculated for the points spanning a vertical section of the experimental channel. The chosen section was over a bed roughened with gravel of nominal diameter 10mm (see [8, 15] for details). The near-bed flow would therefore be expected to show higher turbulence intensity than that remote from the bed. From Figure 3 it may be seen that this is the case. Above  $z/H \approx 0.25$  there is negligible difference

between the despiking methods; closer to the bed VC shows greater disparity with the mPST/PST values, though the difference is still small.

In terms of the power spectra, filtering reduces the energy contained in the high frequency range, as would be expected from the removal of short duration, high magnitude spikes (Figure 4). The differences between the despiking measurements are negligible, and only the mPST-LGV distribution is shown.

### **3.4 The Data of Gunawan et al.**

Application of the despiking methods to the seven data sets of Gunawan et al. allows their comparison when applied to field measurement data from untreated water. As with the data of Jesson et al., PST identifies a higher number of values as being spikes than mPST or VC (Table 5). Once again, PST-LGV detects (though possibly incorrectly) many more spikes than the other methods and is seen to increase  $TI_z$  by 4% relative to mPST-LGV.

The power spectra show negligible variation by despiking method and are not shown.

## **4 Conclusions**

A range of despiking methods (each being a combination of a spike-detection method and a spike-replacement strategy) have been evaluated against velocity time-series from a variety of sources, namely artificially corrupted test data, laboratory flume data measured in clean water, and field experiment data captured in untreated, “dirty” river water. The following conclusions are drawn:

- mPST is recommended due to its computational efficiency accuracy at detecting spikes, especially for large or highly corrupted data sets. However, both PST and VC are satisfactory for the relatively “clean” data sets obtained from laboratory and field experiments
- PST accurately reconstructs the spectral density distribution when used in conjunction with a 12-point polynomial replacement strategy. This is somewhat at odds with the conclusions

of Parsheh et al. who used PST-LGV and concluded that PST did not accurately reconstruct the distribution.

- the recommended replacement method is dependent on the detection method, with LGV preferred for mPST and 12PP for PST due to the improvement these pairings give with reconstruction of the spectral density distribution
- the use of the median absolute deviation as a characteristic scalar is only recommended for highly corrupt data sets where use of the standard deviation fails, as it is shown to incorrectly identify more values as spikes than the standard deviation
- all despiking methods have negligibly differing effects on the turbulence intensity, with the exception of PST-LGV which disproportionately affected the z-component of TI in both sets of experimental data

## **5 Acknowledgements**

The authors would like to thank those researchers who have kindly provided copies of their experimental data.

## **6 Vitae**

Dr Michael Jesson is a Research Fellow with an interest in the practical application of fluid mechanics. He recently finished his PhD, examining turbulence propagation and secondary flow structures in open-channel flow over a laterally heterogeneous bed, and the modelling of such a channel using the Shiono-Knight Method. His current research is investigating thunderstorm downbursts, with the aim of improving their simulation under laboratory conditions and thus our understanding of them; the final goal is to improve the design of buildings and other structures which must withstand these extreme events.

Dr Mark Sterling is currently a Reader in Fluid Dynamics with research interests in Wind Engineering and Water Engineering. His research in Water Engineering is mainly directed towards understanding and evaluating the conveyance capacity of rivers, while within the field of Wind Engineering he has



carved out two distinct areas of research, namely the effect of wind on plants and the effects of extreme wind events. He has have been involved in a variety of research council and industrial funded projects, has a research portfolio in excess of £1,600,000 and has published over 90 journal/conference publications.

Dr John Bridgeman is a Reader in Environmental Engineering. Prior to his appointment at the University of Birmingham in 2005, John spent 15 years working in the water industry on planning, feasibility and detailed process and hydraulic design of water and wastewater treatment systems. He now delivers lectures and workshops at postgraduate and undergraduate levels on topics associated with water treatment processes and water quality, hydraulics, numerical modelling and asset management, and is an active researcher in these fields.

## 7 References

- [1] Tropea C. Laser Doppler anemometry: recent developments and future challenges. *Measurement Science and Technology*. 1995;6:605.
- [2] Goring DG, Nikora VI. Despiking Acoustic Doppler Velocimeter Data. *Journal of Hydraulic Engineering*. 2002;128:117-26.
- [3] Benedict LH, Noback H, Tropea C. Estimation of turbulent velocity spectra from laser Doppler data. *Measurement Science and Technology*. 2000;11:1089-104.
- [4] Lohrmann A, Cabrera R, Kraus NC. Acoustic Doppler Velocimeter (ADV) for Laboratory Use. *Fundamentals and Advancements in Hydraulic Measurements and Experimentation*. Buffalo, New York: ASCE; 1994. p. 351-65.
- [5] Nortek. Vectrino Velocimeter User Guide. Rev C ed: Nortek AS, Vangkroken 2, NO-1351 RUD, Norway; 2004.
- [6] Nikora V, Goring D. Flow turbulence over fixed and weakly mobile gravel beds. *Journal of Hydraulic Engineering*. 2000;126:679-90.
- [7] Vermaas DA, Uijttewaai WSJ, Hoitink AJF. Lateral transfer of streamwise momentum caused by a roughness transition across a shallow channel. *Water Resources Research*. 2011;47:W02530.
- [8] Jesson M, Sterling M, Bridgeman J. An Experimental Study of Turbulence in a Heterogeneous Channel. *Proceedings of the Institution of Civil Engineers, Water Management*. 2012;(In Press).
- [9] Nikora VI, Goring DG. ADV Measurements of Turbulence: Can We Improve Their Interpretation. *Journal of Hydraulic Engineering*. 1998;124:630-4.
- [10] Lane SN, Biron PM, Bradbrook KF, Butler JB, Chandler JH, Crowell MD, et al. Three-Dimensional Measurement of River Channel Flow Processes Using Acoustic Doppler Velocimetry. *Earth Surface Processes and Landforms*. 1998;23:1247-67.
- [11] Jesson M. The Effect of Heterogeneous Roughness on Conveyance Capacity and Application to the Shiono-Knight Method [PhD Thesis]: University of Birmingham, UK; 2012.
- [12] Parsheh M, Sotiropoulos F, Porte-Agel F. Estimation of Power Spectra of Acoustic-Doppler Velocimetry Data Contaminated with Intermittent Spikes. *Journal of Hydraulic Engineering*. 2010;136:368-78.

- [13] Wahl TL. Discussion of "Despiking Acoustic Doppler Velocimeter Data" by Derek G. Goring and Vladimir I. Nikora. *Journal of Hydraulic Engineering*. 2003;129:484-7.
- [14] Cea L, Puertas J, Pena L. Velocity Measurements on Highly Turbulent Free Surface Flow Using ADV. *Experiments in Fluids*. 2007;42:333-48.
- [15] Jesson M, Sterling M, Bridgeman J. Turbulent Structures in Heterogenous Channels and Their Effects on Conveyance. First IAHR European Division Congress. Heriot-Watt University, Edinburgh: IAHR; 2010.
- [16] Rusello PJ. A Practical Primer for Pulse Coherent Instruments, Technical Note TN-027. Nortek AS; 2009.
- [17] Gunawan B, Sun X, Sterling M, Knight DW, Shiono K, Chander JH, et al. An integrated and novel approach to estimating the conveyance capacity of the river Blackwater. *Proceedings of the 8th International Conference on Hydroscience and Engineering (ICHE-2008)*. Nagoya, Japan 2008.
- [18] Nezu I, Nakagawa H. *Turbulence in Open-Channel Flows*. Rotterdam: A.A. Balkema; 1993.

Despiking Method	Standard Deviation	Correctly Replaced Spikes		Missed Spikes		Incorrectly Identified as Spikes	
Uncontaminated	0.9569	N/A		N/A		N/A	
Contaminated	3.2280	(58931)	100%	N/A		N/A	
mPST-12PP	0.9572	58787	99.8%	144	0.0%	214	0.0%
mPST-LGV	0.9567	58785	99.8%	146	0.0%	616	0.0%
mPST-LI	0.9602	58785	99.8%	146	0.0%	92	0.0%
PST- $\vartheta$ -12PP	0.9467	58931	100%	0	0.0%	153084	2.6%
VC-SD-12PP	0.9935	54258	92.1%	4673	0.1%	6	0.0%
VC- $\vartheta$ -12PP	0.9935	55157	93.6%	3774	0.1%	6	0.0%

Table 1: Results of Filtering Application to the Full Data of Parsheh et al. [12]. Percentages are relative to the true number of spikes.

Despiking Method	Standard Deviation	Correctly Replaced Spikes		Missed Spikes		Incorrectly Identified as Spikes	
Uncontaminated	1.0026	N/A		N/A		N/A	
Contaminated	3.2285	(4992)	100%	N/A		N/A	
mPST-12PP	1.0060	4981	99.8%	11	0.0%	28	0.0%
mPST- $\vartheta$ -12PP	1.0053	4981	99.8%	11	0.0%	66	0.0%
mPST-LGV	1.0024	4980	99.8%	12	0.0%	65	0.0%
mPST- $\vartheta$ -LGV	1.0022	4981	99.8%	11	0.0%	73	0.0%
mPST-LI	1.0059	4980	99.8%	12	0.0%	20	0.0%
mPST- $\vartheta$ -LI	1.0035	4981	99.8%	11	0.0%	50	0.0%
PST-12PP	0.9982	4992	100%	0	0.0%	6709	134.4%
PST- $\vartheta$ -12PP	1.0010	4992	100%	0	0.0%	12113	2446.2%
PST-LGV	Failed	N/A		N/A		N/A	
PST- $\vartheta$ -LGV	1.0033	4992	100%	0	0.0%	9403	188.4%
PST-LI	1.0015	4992	100%	0	0.0%	4866	97.5%
PST- $\vartheta$ -LI	1.0014	4992	100%	0	0.0%	6513	130.5%

Table 2: Results of Filtering Application to the Partial Data Set of Parsheh et al. [12]. Percentages are relative to the true number of spikes.

Data Set	Number of Values	Removed Values		$\sigma$			$\theta$ Before
		Count	%age	Before	After	% Reduction	
Parsheh et al. (Full)	1200000	36019	3.0	3.228	1.337	59	1.35
Parsheh et al. (Partial)	100000	3336	3.3	3.228	1.281	60	1.35
Jesson et al	12000	45	0.4	0.087	0.068	12	0.073

Table 3: Data Set Properties Before and After the Automatic Exclusion Step of mPST

<b>Despiking Method</b>	<b>TI<sub>x</sub></b>	<b>TI<sub>y</sub></b>	<b>TI<sub>z</sub></b>	<b>%age Valid</b>
Unfiltered	20	7	2	100
mPST-12PP	-1	-1	0	98
mPST-LGV	0	0	0	97
mPST-LI	-1	0	1	98
PST-12PP	-2	-2	-1	96
PST-LGV	0	1	4	93
PST-LI	-1	-1	0	96
VC-12PP	1	1	1	98
VC-LGV	2	2	2	98
VC-LI	1	1	2	98

**Table 4: Mean Turbulence Intensity (Percentage Difference from mPST-LGV Value) and Percentage of Values Which are Valid by Despiking Method**

<b>Despiking Method</b>	<b>TI<sub>x</sub></b>	<b>TI<sub>y</sub></b>	<b>TI<sub>z</sub></b>	<b>%age Valid</b>
Unfiltered	1	1	2	100
mPST-12PP	0	0	0	99
mPST-LGV	0	0	0	99
mPST-LI	0	0	0	99
PST-12PP	0	0	-1	98
PST-LGV	0	2	4	94
PST-LI	0	0	0	98
VC-12PP	0	0	1	99
VC-LGV	0	0	1	99
VC-LI	0	0	1	99

**Table 5: Mean Turbulence Intensity (Percentage Difference from mPST-LGV Value) and Percentage of Values Which are Valid by Despiking Method**

Figure 1: Illustrative Time-Series: The artificially corrupted data of Parsheh et al. [12] (a); the filtered data of Parsheh et al. [12] (b); unfiltered experimental data of Jesson et al. [8] (c)

Figure 2: Power Spectra for the Despiked Partial Data Set Using PST and mPST

Figure 3: Vertical Distribution of  $TI_x$  by Despiking Method

Figure 4: Power Spectra from the Data of Jesson et al.